

THE RELATIONSHIP BETWEEN RUPTURE LIFE AND CREEP PROPERTIES
OF 2 1/4 Cr-1 Mo STEEL*

R. L. Klueh

Metals and Ceramics Division
Oak Ridge National Laboratory
Oak Ridge, Tennessee 37830

NOTICE

This report was prepared as an account of work sponsored by the United States Government. Neither the United States nor the United States Atomic Energy Commission, nor any of their employees, nor any of their contractors, subcontractors, or their employees, makes any warranty, express or implied, or assumes any legal liability or responsibility for the accuracy, completeness or usefulness of any information, apparatus, product or process disclosed, or represents that its use would not infringe privately owned rights.

ABSTRACT

Several investigators have demonstrated empirical relationships between creep and rupture properties for various metals and alloys. We have examined empirical relationships between the rupture life and the minimum creep rate and the rupture life and the time to the end of steady-state creep (start of tertiary creep) for four heats of normalized-and-tempered 2 1/4 Cr-1 Mo steel with different carbon contents. The primary objective was the determination of the conditions that affect the correlation. The primary microstructural constituent (proeutectoid ferrite or bainite) of the matrix and the precipitates present in that matrix (before test or formed during test) played a significant role in the correlation of the data with the chosen empirical relationship.

INTRODUCTION

Empirical relationships between creep and rupture properties have been shown to exist for several metals and alloys at elevated temperatures [1-5].[†] Figure 1 shows a schematic creep-rupture diagram and

*Research sponsored by the U.S. Atomic Energy Commission under contract with Union Carbide Corporation.

[†]Numbers in brackets designate references at end of paper.

MASTER

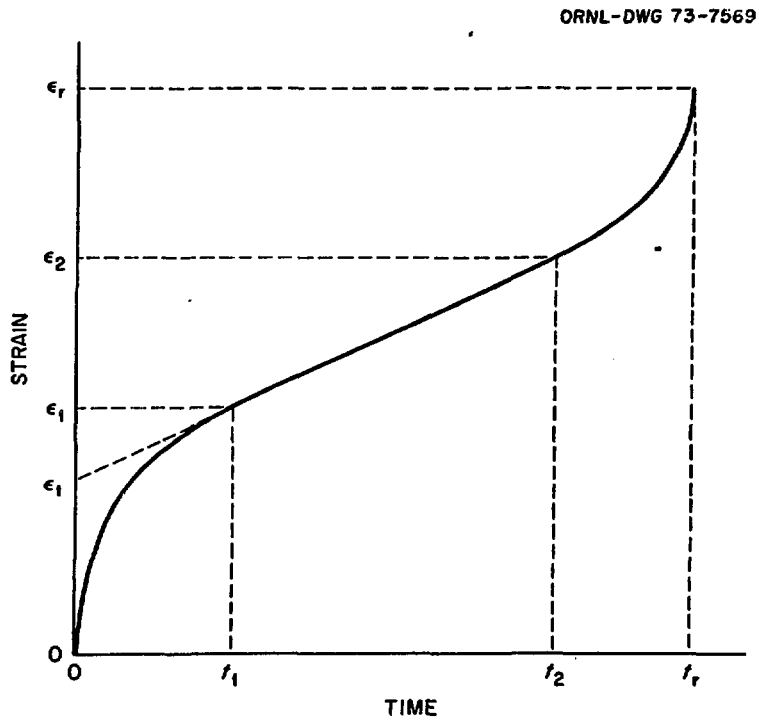


Fig. 1. Schematic Diagram of a "Typical" Creep-Rupture Curve Showing the Three Stages of Creep.

defines the creep and rupture quantities of interest. Monkman and Grant [1] showed that several metals and alloys follow an empirical relationship between rupture time t_r and the steady-state creep rate $\dot{\epsilon}_s$ such that

$$t_r = C/(\dot{\epsilon}_s)^\alpha, \quad (1)$$

where C and α are constants. Several investigators [1-3] have found α to be near unity and assumed C to be independent of temperature and stress. For example, Monkman and Grant [1] tried to fit all ferritic steel data to one curve and found considerable scatter. However, the data included materials with up to 13% Cr and temperatures from 427 to 704°C (800 to 1300°F).

Equation (1) was found by Garofalo et al. [4] to be obeyed by type 316 stainless steel, but in this case C was slightly temperature sensitive. They also found that empirical relationships exist between rupture time and the time to the end of secondary creep (start of tertiary creep), t_2 , and the time spent in secondary creep, $t_2 - t_1$; namely,

$$t_r = B(t_2 - t_1)^\gamma, \quad (2)$$

and

$$t_r = A(t_2)^\beta, \quad (3)$$

where t_1 is the time to the end of transient creep and A , B , β , and γ are constants, with β and γ near unity. However, at the higher test temperatures where deviations from Eq. (1) were noted for long-time tests,

Garofalo et al. [4] found that Eqs. (2) and (3) were still obeyed. The deviation from Eq. (1) was attributed to the nature of the grain boundary precipitate.

Following Garofalo et al. [4], Fig. 1 shows that

$$\dot{\epsilon}_s = \frac{\epsilon_2 - \epsilon_1}{t_2 - t_1} = \frac{\epsilon_2 - \epsilon_t}{t_2} \quad , \quad (4)$$

Substitution of Eq. (4) into (2) and (3) gives

$$t_r = A \left(\frac{\epsilon_2 - \epsilon_t}{\dot{\epsilon}_s} \right)^\beta \quad , \quad (5)$$

and

$$t_r = B \left(\frac{\epsilon_2 - \epsilon_1}{\dot{\epsilon}_s} \right)^\gamma \quad , \quad (6)$$

thus indicating a relationship between elongation and C of Eq. (1). For an α , β , and γ of unity, Eqs. (1), (5), and (6) indicate that the product of the rupture time and minimum creep rate is a constant and some function of the elongation during the secondary stage of creep [2,4]. Although Garofalo et al. [4] found $\epsilon_2 - \epsilon_1$ to be a constant when Eq. (1) applied, other investigators [1] have been unable to establish a relationship between a measure of creep elongation and C .

The ferritic 2 1/4 Cr-1 Mo steel has wide application in the chemical process and petroleum industries and in power-generating equipment. At present much of the available high-temperature data is creep-rupture data that was collected at stresses above those of direct interest for design purposes. Analysis of these data is important, however, for the information that can be derived relative to creep behavior, especially

any trends that may be detected with decreasing stress. Furthermore, much of the data obtained for use in setting ASME Boiler and Pressure Vessel Code Case allowable stresses are from rupture studies. Thus, any information derived relative to the applicability of empirical relationships to 2 1/4 Cr-1 Mo steel should find practical application. In the present paper, we have analyzed data on selected heats of 2 1/4 Cr-1 Mo steel to determine the conditions under which the empirical relationships discussed above are applicable.

EXPERIMENTAL

We have previously reported on the metallography and mechanical properties of four heats of 2 1/4 Cr-1 Mo steel with varying carbon contents [6]. Three of the heats were 300-lb heats melted, cast, and fabricated into 7/8-in. rods and contained 0.009, 0.030, and 0.120% C (the last was a remelted commercial heat). The fourth steel was a 1-in. plate of a commercial heat with 0.135% C. Since the details on the materials and the creep-rupture test procedures were previously given [6], they will not be further discussed.

The tests were conducted on the steels in the normalized-and-tempered condition: 1 hr at 927°C (1700°F), air-cooled, 1 hr at 704°C (1300°F), air cooled (the steels were heat treated as 7/8-in. rods or 1-in. plate). In this condition, the carbon content determined the primary microstructural constituents: the 0.009 and 0.030% C steels were primarily proeutectoid ferrite, containing 1-2 and 10-15% bainite, respectively; the 0.120 and 0.135% C steels were entirely bainite. Creep-rupture tests were made at 454, 510, and 565°C (850, 950, and 1050°F). Since in some instances the amount of prestrain on load

appeared to affect some of the creep properties, the yield stresses for the test materials are given in Table 1.

RESULTS

Consider first the data for the 0.009% C steel in Table 2. In general, ϵ_1 and ϵ_t appear to decrease with decreasing stress. The percent decrease in ϵ_1 and ϵ_t with decreasing stress seems to increase significantly at the lowest stresses at 565 and 510°C. No such effect is noted at 454°C, where all tests are above the yield stress and involve considerable prestrain. At 510 and 565°C, both ϵ_2 and $\epsilon_2 - \epsilon_1$, the elongation during secondary creep, show considerable scatter, while at 454°C, they are somewhat more constant.

For the data from the 0.030% C steel in Table 3, similar observations follow. However, for this material all tests at 454 and 510°C were above the yield stress, as were the tests at 22.5 and 25 ksi at 565°C. As observed for the 0.009% C steel, ϵ_2 and $\epsilon_2 - \epsilon_1$ are relatively constant, though with somewhat different values above and below the yield stress. The only exception to this is the 565°C test at 13 ksi. In this case, when the stress was changed but 2 ksi, an order of magnitude decrease was observed in ϵ_t , ϵ_1 (similar to the large decrease noted for ϵ_t and ϵ_1 for the 0.009% C steel), ϵ_2 , $\epsilon_2 - \epsilon_1$. The reason for this change is obvious when the creep curve for this specimen, Fig. 2, is examined; this specimen did not display a "typical" creep curve of the type shown in Fig. 1. After about 300 hr, the steel apparently went into tertiary creep (the t_2 and ϵ_2 values recorded in Table 2), in that the creep rate began to increase with time. After about 550 hr, however, another period of "steady state" creep ensued

Table 1. Yield Stress of 2 1/4 Cr-1 Mo Steels Tested^a

Carbon Content (wt %)	Yield Stress, ksi			Yield Stress, MPa		
	454°C	510°C	565°C	454°C	510°C	565°C
0.009	29.2	23.6	21.4	201	163	148
0.030	26.0	25.6	20.5	179	177	141
0.120	58.3	58.1	54.7	402	401	377
0.135	67.4	71.2	57.8	465	491	399

^aTaken from ORNL-4922.

Table 2. Creep and Creep-Rupture Data for 2 1/4 Cr-1 Mo Steel with 0.009% C

Stress		Primary Creep			Secondary Creep			Tertiary Creep	
(ksi)	(MPa)	ϵ_1 (%)	ϵ_t (%)	t_1 (hr)	ϵ_2 (%)	t_2 (hr)	ϵ_s (%/hr)	ϵ_r (%)	t_r (hr)
<u>565°C (1050°F)</u>									
25	172	1.0	0.45	0.3	2.0	3.5	1.38	23.0	5.6
22.5	155	1.05	0.50	0.5	4.25	2.8	1.35	38.2	8.7
20	138	0.16	0.10	1.0	0.75	9	0.065	19.5	33.6
15	103	0.51	0.29	16.5	1.0	53	0.014	27.0	429.2
12.5	86	0.05	0.02	3.0	0.40	57	0.0065	31.0	797.7
<u>510°C (950°F)</u>									
42.5	293	4.0	1.8	1.6	6.0	3.0	1.2	33.6	5.5
40	276	2.3	1.2	2.2	10.0	5.5	0.525	35.6	15.4
35	241	1.1	0.90	4.0	2.8	32.5	0.0575	30.8	84.4
30	207	0.43	0.35	12.0	1.0	73	0.0096	38.0	262.0
27.5	189	0.38	0.23	50.0	0.5	75	0.0030	32.0	354.4
25	172	0.05	0.02	5.0	0.3	230	0.00125	38.0	672.5
<u>454°C (850°F)</u>									
50	345	2.1	1.4	0.75	4.45	3.2	0.935	28.0	4.1
49	338	3.1	1.5	7.5	6.1	22	0.210	31.0	32.6
47.5	327	2.2	1.3	12.5	7.2	80	0.075	32.5	120.0
45	310	1.95	1.25	21	4.85	100	0.034	30.4	181.5
42.5	293	1.3	1.0	28	3.75	240	0.011	30.4	560.5
41	283	1.7	0.95	75	3.9	310	0.0093	30.4	655.3
41	283	1.5	1.0	70	4.0	410	0.0073	32.0	817.1

Table 3. Creep and Creep-Rupture Data for 2 1/4 Cr-1 Mo Steel
with 0.030% C

Stress		Primary Creep			Secondary Creep			Tertiary Creep	
(ksi)	(MPa)	ϵ_1 (%)	ϵ_t (%)	t_1 (hr)	ϵ_2 (%)	t_2 (hr)	ϵ_S (%/hr)	ϵ_r (%)	t_r (hr)
<u>565°C (1050°F)</u>									
25	172	4.2	1.6	1.5	10.1	5.0	1.75	43.0	10.1
22.5	155	4.4	2.0	7.5	12.5	34	0.308	41.6	65.8
20	138	1.5	0.55	15	6.5	89	0.063	45.6	214.5
20	138	2.9	1.0	20	8.5	93	0.075	43.6	221.8
17	117	1.3	0.50	27	3.3	95	0.029	47.8	536.3
15	103	1.7	0.45	53	5.0	200	0.023	37.1	675.0
13	90	0.1	0.062	15	0.5	160	0.0026	44.8	2062.9
<u>510°C (950°F)</u>									
48	331	4.0	3.0	6.5	7.5	30	0.150	30.4	37.7
47.5	327	3.5	2.75	7.5	9.0	50	0.117	32.0	59.1
45	310	2.4	1.9	17	4.4	83	0.029	36.0	274.5
40	276	2.1	1.38	70	7.5	640	0.0097	31.2	1212.7
40	276	1.5	1.25	30	4.8	350	0.010	33.2	1069.3
35	241	2.8	1.0	575	5.7	1675	0.0028	33.2	2807.9
<u>454°C (850°F)</u>									
56.75	391.3	5.8	3.6	100	8.7	275	0.0165	28.8	332.0
56.70	390.9	7.7	6.9	400	8.0	530	0.0020	30.4	934.3
56.65	390.6	6.5	4.9	620	7.4	960	0.0026	30.4	1560.0
56.50	389.6	5.2	3.3	410	7.5	920	0.0046	29.6	1219.9
56.00	386.1	4.0	2.7	1150	6.1	2900	0.0012	37.0	3776.8
55.00	379.2	4.7	3.4	1600	5.7	2800	0.0008	32.6	3932.6

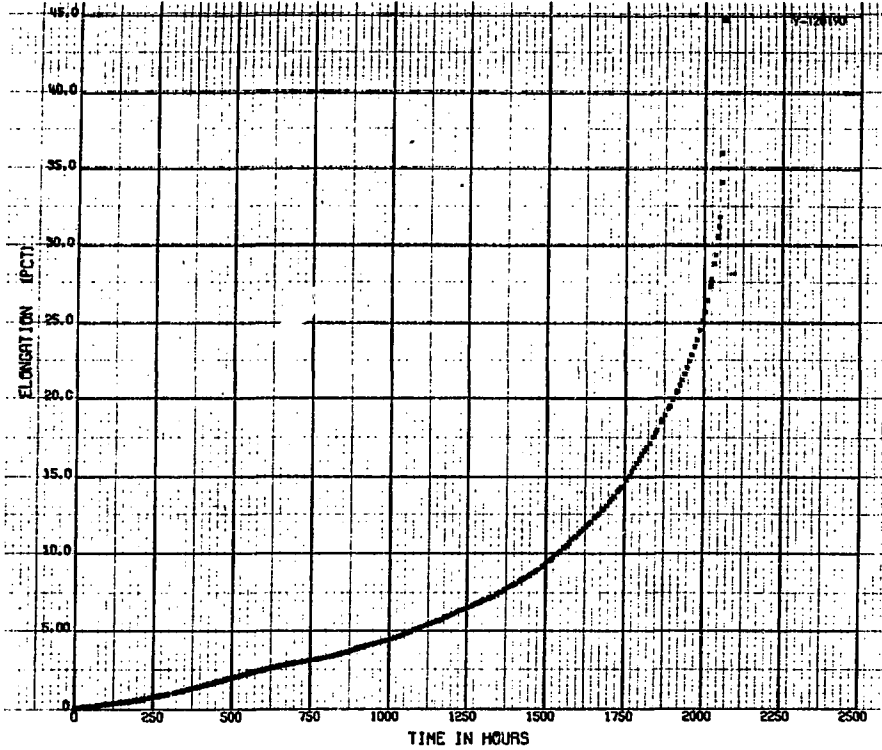


Fig. 2. The Creep-Rupture Curve for the 0.030% C Steel Tested at 565°C and 13,000 psi (90 MPa).

(at a slightly increased rate) out to about 850 hr, after which the creep rate again began to increase and increased to rupture. When ϵ_2 and $\epsilon_2 - \epsilon_1$ at 850 hr are compared with those for the specimens tested at the higher stresses, the relative constancy of these quantities is maintained. We previously pointed out the types of precipitation reactions that occur in 2 1/4 Cr-1 Mo steels [6]. As discussed below, we believe these reactions occurring during test must give rise to the kind of creep curve shown in Fig. 2.

In Figs. 3 and 4 the data for the 0.009 and 0.030% C steels at all three temperatures are plotted in accordance with Eqs. (1) and (2): $\log t_p$ is plotted against $\log \dot{\epsilon}_s$ [Figs. 3(a) and 4(a)] and against $\log t_2$ [Figs. 3(b) and 4(b)]. Although best-fit straight lines have been drawn through the data, the lack of statistical experiments hinders the interpretation.

In Fig. 3(a) for the 0.009% C steel, only one straight line was drawn for the $\log t_p$ vs $\log \dot{\epsilon}_s$ data. Although it was drawn to fit the 454°C data, with three exceptions, the remainder of the data also fall rather nicely on the line with α very near unity. For the 0.030% C steel, on the other hand, lines with α approaching unity were drawn for the data at 454 and 565°C. The data at 510°C, however, appear to have considerable scatter: the short-time data fall on the 454°C line, while the longer time data fall on the 565°C line.

Figures 3(b) and 4(b) show the data plotted in accordance with Eq. (2). Only one best-fit straight line has been drawn, and although there is some scatter, the data fit this curve quite well with β very near unity. These results indicate that the percent of the test time spent in the primary and secondary stages of creep is relatively constant

ORNL-DWG 73-12680R

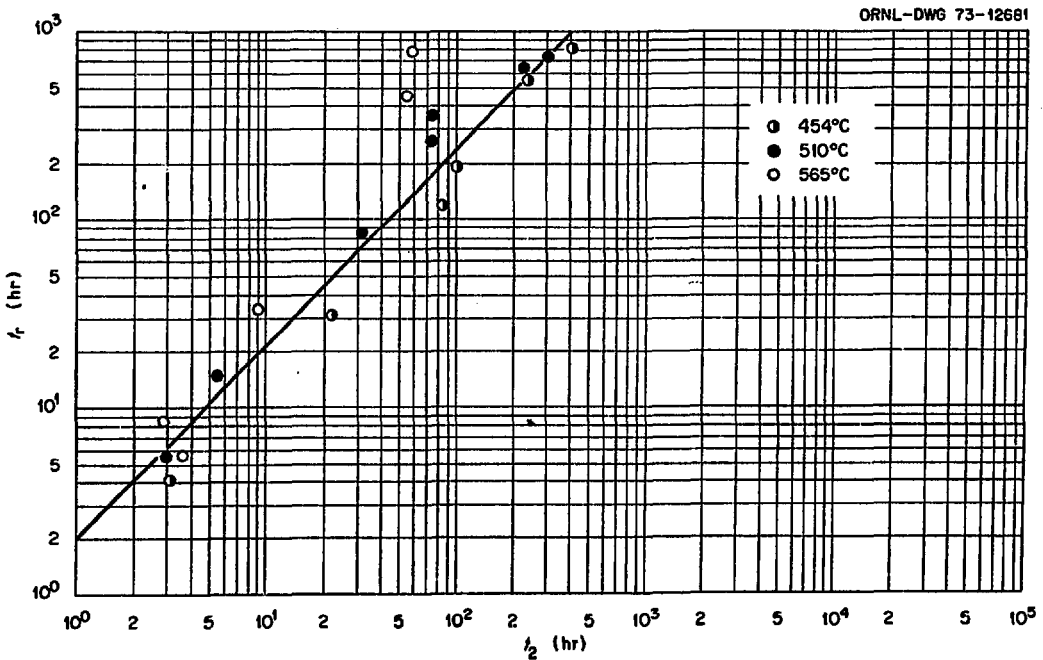
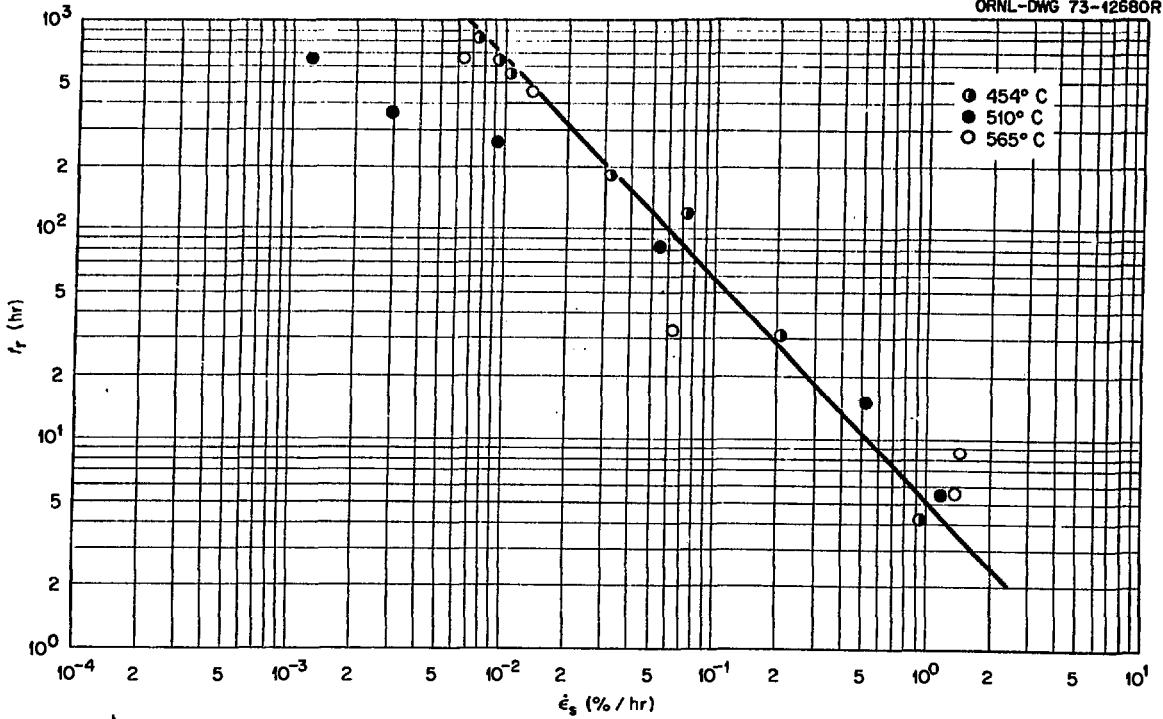


Fig. 3. Relationships Between Rupture Life and (a) Minimum Creep Rate and (b) End of Secondary Creep Stage for 2 1/4 Cr-1 Mo Steel With 0.009% C.

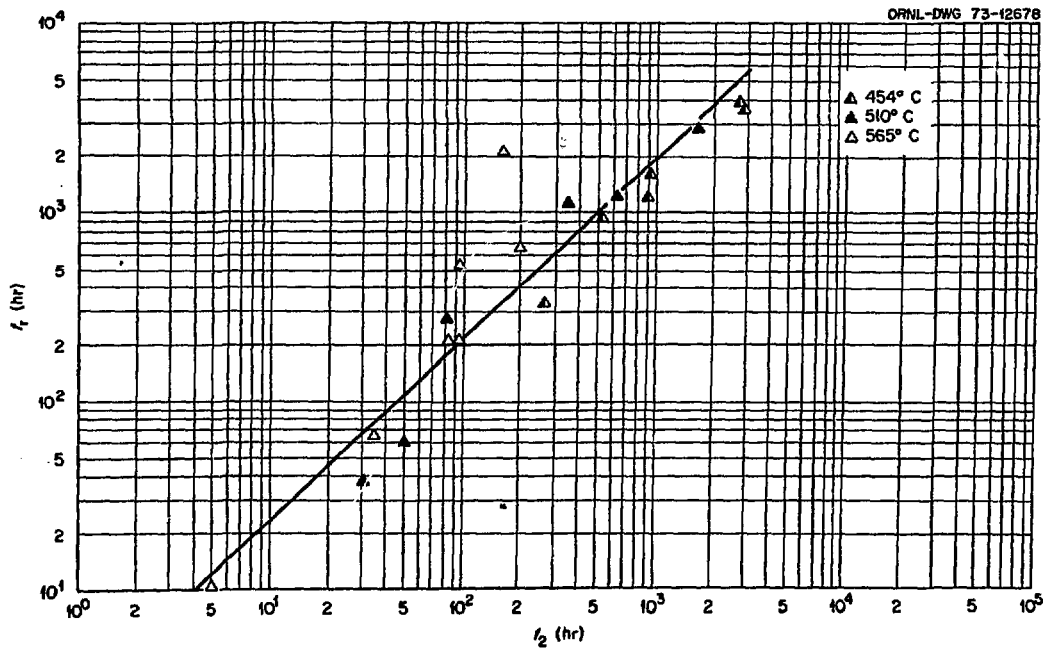
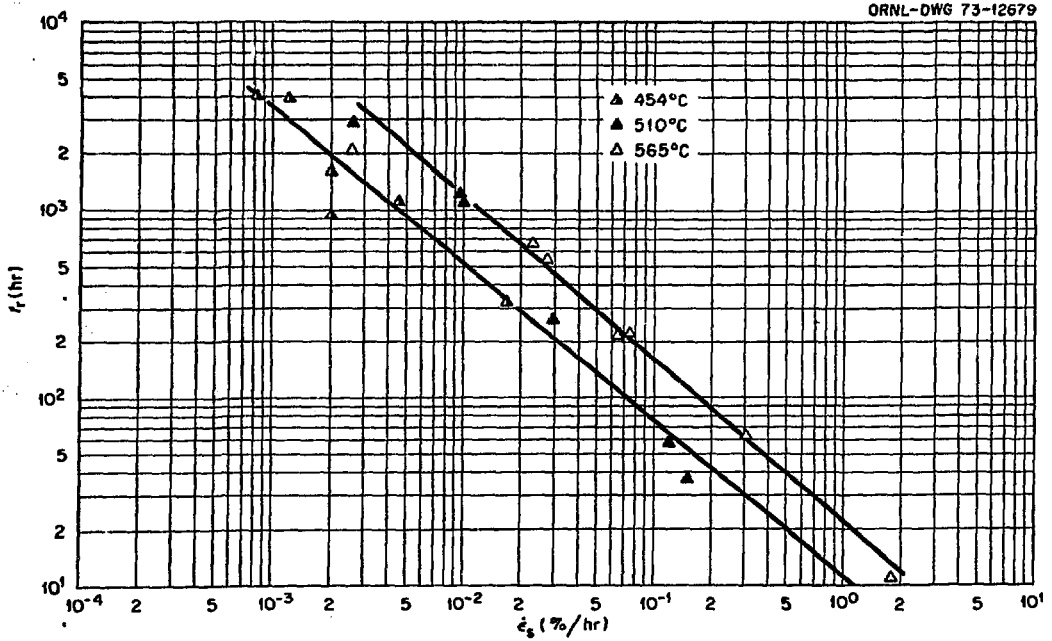


Fig. 4. Relationship Between Rupture Life and (a) Minimum Creep Rate and (b) End of Secondary Creep Stage for 2 1/4 Cr-1 Mo Steel With 0.030% C.

with little dependence on temperature and stress. The only real exceptions to this are the longer time tests at 565°C, and examination of the respective creep curves indicates that they are of the type shown in Fig. 2. Also, a superposition of the t_p , t_2 curves for the 0.009 and 0.030% C steels indicates that the data for both follow a similar relationship (i.e., similar B and β).

We now turn to the data for the two completely bainitic steels with commercial carbon contents (Tables 4 and 5). At 565°C, where all tests were at stresses below the yield stress, ϵ_1 , ϵ_t , ϵ_2 , and $\epsilon_2 - \epsilon_1$ show little change with stress, despite the fact that there was a change in fracture mode — from intergranular to transgranular — that resulted in a slope change in the creep-rupture curve and a change in the rupture elongation, ϵ_p [6]. At 510°C, there is considerable data scatter, and, as pointed out below, this may result from precipitation reactions that are occurring at this temperature (all tests for the 0.135% C steel and all but one for the 0.120% C steel) are at stresses below the yield stress). At 454°C the results of Table 4 for the 0.120% C steel (all tests above the yield) show a slightly decreasing ϵ_1 and ϵ_t when the stress decreases. Somewhat similar conclusions follow for the 0.135% C steel of Table 5 (the 75 and 79 ksi tests are above the yield, though 70 ksi is very near the yield). The three low-stress tests show a relatively constant ϵ_1 , ϵ_t , ϵ_2 , and $\epsilon_2 - \epsilon_1$, while the 79 and 75 ksi tests show higher values, and the results of the 70 ksi test fall in between.

In Fig. 5(a) the data for all three temperatures for the 0.120 and 0.135% C steels are plotted according to Eq. (1). Figure 5(b) shows the combined data represented according to Eq. (2) in a $\log t_p$, $\log t_2$ plot.

Table 4. Creep and Creep-Rupture Data for 2 1/4 Cr-1 Mo Steel
with 0.120% C

Stress		Primary Creep			Secondary Creep			Tertiary Creep	
(ksi)	(MPa)	ϵ_1 (%)	ϵ_t (%)	t_1 (hr)	ϵ_2 (%)	t_2 (hr)	ϵ_s (%/hr)	ϵ_r (%)	t_r (hr)
<u>565°C (1050°F)</u>									
45	310	0.05		0.1	2.0	0.5	3.75	24.1	1.3
35	241	2.15	1.6	4.0	3.8	18	0.14	25.1	32.4
35	241	0.63	0.38	1.7	2.8	12	0.19	28.1	25.0
30	207	0.75	0.35	14	2.8	88	0.026	25.3	194.5
30	207	0.75	0.30	20	2.8	120	0.021	32.8	254.3
25	172	0.44	0.30	19	1.9	160	0.007	24.2	435.9
20	138	0.73	0.45	175	2.0	850	0.0016	14.9	2519.5
<u>510°C (950°F)</u>									
60	414	1.80	1.35	0.25	3.10	1.3	1.55	24.0	2.9
55	379	0.43	0.25	0.75	1.53	6	0.210	26.8	13.4
50	345	0.15	0.1	2.0	0.95	34	0.025	28.0	104.3
45	310	0.08	0.06	0.5	0.23	16	0.012	31.6	173.5
40	276	0.03	0.01	2.5	0.50	100	0.005	28.4	829.9
<u>454°C (850°F)</u>									
75	517	0.6	0.45	1.3	0.85	3.3	0.135	23.9	18.0
70	483	0.5	0.30	5	1.45	59	0.0195	22.0	136.9
67.5	465	0.39	0.21	20	0.80	62	0.0089	19.2	242.9
65	448	0.33	0.23	83	0.89	345	0.0020	19.3	707.5

Table 5. Creep and Creep-Rupture Data for 2 1/4 Cr-1 Mo Steel
with 0.135% C

Stress		Primary Creep			Secondary Creep			Tertiary Creep	
(ksi)	(MPa)	ϵ_1 (%)	ϵ_t (%)	t_1 (hr)	ϵ_2 (%)	t_2 (hr)	ϵ_s (%/hr)	ϵ_r (%)	t_r (hr)
<u>565°C (1050°F)</u>									
45	310	0.37	0.15	0.2	2.25	1.8	1.10	18.5	3.8
40	276	0.77	0.4	1.25	2.75	9	0.30	21.0	15.4
40	276	0.80	0.32	2.5	2.25	10.5	0.19	23.1	22.0
35	241	1.0	0.54	8.8	2.40	30	0.052	22.1	86.1
30	207	0.5	0.22	27	2.00	150	0.0102	15.7	362.2
25	172	0.75	0.36	125	2.00	370	0.0030	15.2	1020.9
<u>510°C (950°F)</u>									
59	407	0.16	0.1	1.2	0.48	7	0.064	22.4	28.5
55	379	0.75	0.53	3.0	1.05	7.5	0.070	23.2	36.8
50	345	0.10	0.04	4	0.26	25	0.013	27.2	130.0
50	345	0.28	0.15	11	0.72	49	0.011	24.1	181.7
47	324	0.30	0.25	6	0.95	104	0.0075	25.1	428.1
45	310	0.10	0.06	4	0.96	106	0.0080	26.4	416.0
40	276	0.65	0.30	100	1.10	300	0.0024	20.8	1558.9
35	241	0.40	0.20	200	1.90	1400	0.001	19.4	4133.5
<u>454°C (850°F)</u>									
79	545	0.52	0.38	0.8	1.70	8	0.164	18.0	14.4
75	517	0.88	0.50	8	1.63	25	0.044	18.4	53.5
70	483	0.30	0.22	8	0.72	45	0.0115	16.8	125.0
66	455	0.10	0.08	15	0.35	210	0.0013	18.4	542.3
65	448	0.18	0.097	50	0.45	210	0.0016	20.0	513.3
64	441	0.11	0.09	25	0.29	295	0.00086	20.1	831.1

Two straight lines have been shown on Fig. 5(a). All the 565°C data and the long-time tests at 510°C fall on one line, while all the 454°C data and the short-time tests at 510°C fall on the other line. Again the slopes of the two curves are such that α is very near unity. The largest deviation of α from unity is observed for the 0.135% C steel at 454°C, primarily because of the three long-time data points. In Fig. 5(a) these points were ignored. Note that despite a change in fracture mode (from transgranular to intergranular) at 565°C, there is no apparent effect on the fit of the data in Fig. 5.

In Fig. 5(b) the data for both steels are given in one $\log t_r$, $\log t_2$ plot. With the exception of several of the 510°C tests, which fall to the left of the curve, the data follow one straight line with β near unity. When the creep curves for the tests that deviate from the curves were examined, it was quite obvious that they exhibited "atypical" creep curves similar to that of Fig. 2. If the time to the end of the second "steady-state" period is taken for t_2 , the agreement with the remainder of the data is excellent.

Tables 6 and 7 give the coefficients for the least squares lines for the data shown in Figs. 3 through 5, as determined from Eqs. (1) and (2). For the t_r , $\dot{\epsilon}_s$ relationships of Table 6, the insufficiency of data hinders the usefulness of the relationships. Nevertheless, the approach of α to unity for most of the data is apparent. Where two sets of coefficients are given, the second was determined after a point that obviously deviated was dropped. The combined curve [shown in Fig. 5(a)] for the 0.120 and 0.135% C steel was determined without the three long-time tests for the 0.135% C steel.

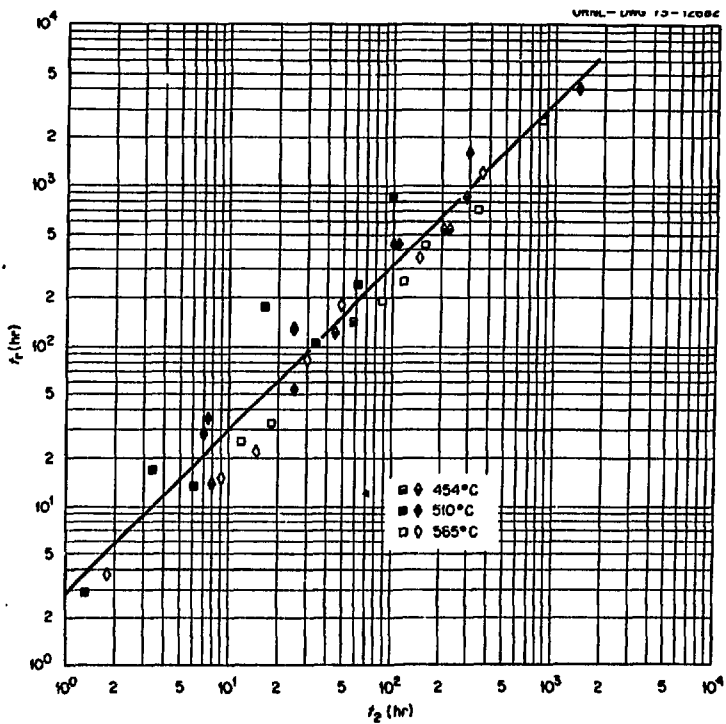
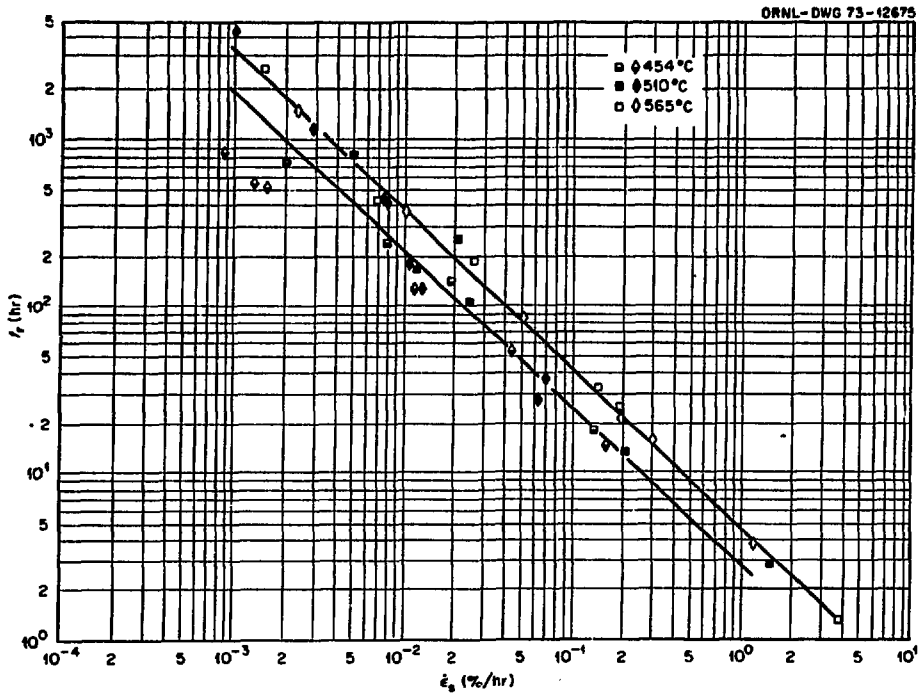


Fig. 5. Relationships Between Rupture Life and (a) Minimum Creep Rate and (b) End of Secondary Creep Stage for Both the 0.120 and 0.135% C Steels.

Table 6. Coefficients for Empirical Relationship Between Rupture Life and Minimum Creep Rate

Carbon (wt %)	Temperature (°C)	Number of Data	α	C	SE ^a
0.009	454	7	1.05	0.719	0.11
0.030	454	6	0.80	1.11	0.17
		5 ^b	0.84	1.05	0.07
0.030	565	7	0.83	1.35	0.13
		6 ^b	0.95	1.26	0.05
0.120	454	4	0.87	0.56	0.09
0.135	454	6	0.74	0.67	0.06
0.120 and 0.135	454	8	0.92	0.46	0.09
0.120	565	7	0.97	0.70	0.08
0.135	565	6	0.95	0.67	0.04
0.120 and 0.135	565	13	0.96	0.67	0.07

^aStandard error of estimate.

^bOne obviously deviating point excluded.

Table 7. Coefficient for Empirical Relationship Between Rupture Life and Time to the Start of Tertiary Creep

Carbon (wt %)	Number of Data	β	A	SE ^a
0.009	17	1.04	0.29	0.27
0.030	18	0.93	0.45	0.19
0.009 and 0.030	35	0.97	0.38	0.23
0.120 and 0.135	36	1.01	0.46	0.19

^aStandard error of estimate.

The t_p , t_2 relationships of Table 7, where the data from all temperatures are rather closely accommodated by one curve, indicate that β approaches unity in all cases. All data were included in fitting the curves of Table 7, and no attempt was made to improve the fit for the points that obviously deviate from the majority of the data and can be accounted for by "atypical" creep curves. As stated before, superposition of the curves for the 0.009 and 0.030% C steels indicated good agreement. To verify that a common equation could be used to represent these data, we plotted the 95% joint confidence ellipses about the estimated equation parameters. Such a plot showed a large region common to both data sets and implies that the data may be represented by a common equation. (If the two ellipses did not overlap, the data should not be combined.) On the other hand, a superposition of the curve for the 0.120 and 0.135% C steels on the curve for the 0.009 and 0.030% C steels shows that it is shifted slightly to the right of the curves for the other two steels. When the joint confidence ellipses for both combined data sets are plotted, only a small region of overlap was found. Although this smaller region indicates a shift in the data, the overlap implies that a single equation may be used to represent the data, an indication that A may be insensitive to a difference in the primary microstructural constituent (proeutectoid ferrite and bainite). Without further data, however, we have not chosen to write an equation for all data.

704°C, but optimum strengthening (as measured by hardness) requires between 1 and 10 hr at 704°C and longer at lower temperatures. We also know that overaging occurs first in the low-carbon steel.

All indications are that the 0.009% C steel quickly overages at 565°C, and overaging was complete before the test was begun [6]. The strength at 565°C is therefore characteristic of the ferrite matrix. With the exception of three tests at 510°C, the remainder of the tests shown in Fig. 3(a) fall on the straight line with the 565°C data. Hence, the small amount of precipitate formed in this low-carbon steel at 704°C must not affect the strength (i.e., at all temperatures, the strength is characteristic of the ferrite).

The data for the 0.030% C steel in Fig. 4(a) appear somewhat more complicated. The same precipitation reaction occurs, but because of the increased carbon content, the time period over which it occurs at a given temperature will increase over that for the 0.009% C steel. We have previously used the precipitation reactions to explain the similarity of the creep-rupture properties of the 0.030% C steel and those of the 0.120 and 0.135% C steels at 454 and 510°C [6]. We will here rely on the same explanation, although verification in both instances awaits electron microscopy studies.

At the highest test temperature, 565°C, the Mo₂C has little effect on the strength, probably because the Mo₂C precipitate particles have grown to such an extent that the interparticle spacing is too large to appreciably enhance the strength much over that of the ferrite matrix. At 454°C, on the other hand, the creep rate and its relationship to rupture life is affected by the Mo₂C that formed during the temper.

The two parallel curves, therefore, represent these two microstructural extremes: dispersion-strengthened ferrite at 454°C, unstrengthened ferrite at 565°C. Finally, at 510°C, where a line through the data would approach the 454°C line for short rupture times and approach the 565°C line for long rupture times, the temperature is such that the short-time rupture properties are determined by the Mo₂C-strengthened ferrite, and the data fall on the 454°C curve, while the long-time rupture properties are those determined by the unstrengthened (overaged) matrix, and the data fall on the 565°C curve.

In Fig. 3(a) for the 0.009% C steel, three of the long-time tests at 510°C deviate from the indicated curves. Likewise, in Fig. 4(a) for the 0.030% C steel, two long-time tests deviate -- one at 510°C, one at 565°C. Although we feel that these deviations, which are of the type found by Garofalo et al. [4], involve precipitation, perhaps M₆C formation, electron microscopy is required for verification.

The explanation for the two straight lines for the $\log t_r$, $\log \dot{\epsilon}_s$ representation for the 0.120 and 0.135% C steels is again sought in the carbide precipitates. In bainite, the Mo₂C again enhances the creep-rupture strength, but it is much more quickly replaced by other carbides that have little or no effect on creep strength. Hardness measurements indicated that the maximum strengthening effect for Mo₂C in these steels is exceeded during the 704°C temper, although considerable Mo₂C is still present in the microstructure after the temper [6]. Therefore, the 454 and 565°C curves in Fig. 5(a) must represent different stages in the overaging process. That is, since the overaging proceeds much more quickly, the higher the temperature, the 565°C curve must represent material that is little affected by Mo₂C, while the 454°C curve represents material still

strengthened by the Mo_2C formed during tempering. The transition from one curve to the other occurs at 510°C , where, given enough time, overaging proceeds to such an extent that the properties are similar to those at 565°C , while for shorter rupture times, they correspond to those at the lower temperature.

With three exceptions, both materials follow the same $t_p, \dot{\epsilon}_s$ relationships [Fig. 5(a)]. The exceptions are the three long-time tests for the 0.135% C steel at 454°C . At present, no logical explanation for this deviation is available. All three of these tests were below the yield stress, but all 510°C tests, which follow the relationship, were also below the yield. Since these tests appear to fit the t_p, t_2 relationship [Fig. 5(b)], whatever causes the deviation affects t_2 and t_p similarly. It must again be the result of precipitate reactions, but further electron microscopy is required. These points were ignored in the curve drawn in Fig. 5(a).

Grant [5] has defined ϵ_2 , the total elongation during the primary and secondary stages of creep, as the "true elongation" because: "the useful life of a metal ends when the first cracks appear or when distinct diminution of the cross section occurs" As we have seen in this study, however, the end of secondary creep, as normally defined (increasing creep rate), does not always coincide with neck or crack formation. Although we have not verified it, we feel the t_2 that fits Eq. (2) is the one defined by Grant [5], while the premature t_2 of "atypical" creep curves (end of first "steady-state" period) is not indicative of the end of the useful life.

Several investigators have pointed out that the constant C of Eq. (1) is related to some measure of elongation, but with the exception

of Garofalo et al. [4], have not determined a relationship [1]. Although our data show some indication of a constancy of $\epsilon_2 - \epsilon_1$, the scatter is too great to verify any relationship to C .

SUMMARY AND CONCLUSION

We have collated and plotted data from four heats of normalized-and-tempered 2 1/4 Cr-1 Mo steel according to empirical relationships between rupture life and minimum creep rate and rupture life and the time to tertiary creep. The primary objective of this paper was not the determination of a curve or curves for 2 1/4 Cr-1 Mo steel that could be used under all conditions. Rather, we were interested in determining what the limitations were on the use of these equations and what refinements might be made to improve their usefulness. Toward that end, we showed that precipitation processes occurring during test influence the fit of the empirical equations. When these precipitation reactions are taken into account, the degree of correlation is considerably improved. As a result, we suggest that whenever such correlations are of interest, it is most useful to have a detailed understanding of the metallurgy of the materials under study. By understanding the material, it may also prove possible to explain the large amount of scatter often found when a large data set obtained from various sources is represented according to these empirical equations.

ACKNOWLEDGMENTS

The author gratefully acknowledges T. E. Hebble for making the statistical calculations; W. R. Martin, R. W. Swindeman, and E. E. Bloom

for helpful discussions on the manuscript; Sigfred Peterson for a review of the manuscript; and Rhonda Castleberry of the Reports Office for preparing the manuscript.

REFERENCES

1. Monkman, F. C., and Grant, N. J., "An Empirical Relationship Between Rupture Life and Minimum Creep Rate," *Proceedings of the ASTM*, Vol. 56, 1956, pp. 593-605.
2. Davies, P. W., and Wilshire, B., "An Interpretation of the Relationship Between Creep and Fracture," *Structural Processes in Creep*, Iron and Steel Institute, London, 1961, pp. 34-43.
3. Servi, I. S., and Grant, N. J., "Creep and Stress-Rupture Behavior of Aluminum as a Function of Purity," *Transactions of the AIME*, Vol. 191, No. 10, Oct. 1951, pp. 909-916.
4. Garofalo, F., et al., "Creep and Creep-Rupture Relationships in an Austenitic Stainless Steel," *Transactions of the AIME*, Vol. 310, No. 4, Apr. 1961, pp. 310-319.
5. Grant, J. M., "Stress Rupture Testing," *High Temperature Properties of Metals*, American Society for Metals, Cleveland, 1951, pp. 41-72.
6. Klueh, R. L., *Effect of Carbon on the Mechanical Properties of 2 1/4 Cr-1 Mo Steel*, ORNL-4922, Nov. 1973.
7. Baker, R. S., and Nutting, J., "The Tempering of 2 1/4% Cr-1% Mo Steel After Quenching and Normalizing," *Journal of the Iron and Steel Institute*, Vol. 192, July 1959, pp. 257-268.

LIST OF FIGURES

Fig. 1. Schematic Diagram of a "Typical" Creep-Rupture Curve Showing the Three Stages of Creep.

Fig. 2. The Creep-Rupture Curve for the 0.030% C Steel Tested at 565°C and 13,000 psi (90 MPa).

Fig. 3. Relationships Between Rupture Life and (a) Minimum Creep Rate and (b) End of Secondary Creep Stage for 2 1/4 Cr-1 Mo Steel With 0.009% C.

Fig. 4. Relationship Between Rupture Life and (a) Minimum Creep Rate and (b) End of Secondary Creep Stage for 2 1/4 Cr-1 Mo Steel With 0.030% C.

Fig. 5. Relationships Between Rupture Life and (a) Minimum Creep Rate and (b) End of Secondary Creep Stage for Both the 0.120 and 0.135% C Steels.